Science & Technology Development Journal 2025, 28(4):3849-3856
Open Access Full Text Article

Review Article

The contributing components of BR $(\mu \to e\gamma)$ in the 3-3-1 model with inverse seesaw neutrinos

H. T. HUNG[1,*], N. T. T. HANG[2], P. T .GIANG[3]

Use your smartphone to scan this

ABSTRACT
The 3-3-1 model with inverse seesaw neutrinos (331 ISS) explains the experimental data of neutrinos very well. Based on the lepton flavor violation sources (presented in Yukawa interactions) and kinetic energy terms, we have shown the couplings involving charged bosons ($W^{\pm}$, $Y^{\pm}$, $H_1^{\pm}$, $H_2^{\pm}$). We also show the analytical results of all the one-loop order contributions to the $\mu \to e\gamma$ decay. We compare the contributions through numerical results and show that the parameter space region of the model satisfies the experimental constraints of $\mu \to e\gamma$ decay.
Key words: Lepton flavor violating decay, Extensions of electroweak Higgs sector, Rare decay, Electroweak radiative corrections, Neutrino mass, and mixing, etc...

[1]*Department of Physics, Hanoi Pedagogical University 2, Xuan Hoa, Phu Tho, Vietnam*

[2]*The University of Fire Prevention and Fighting, 243 Khuat Duy Tien, Dai Mo, Hanoi, Vietnam*

[3]*Basic Faculty, Vietnam Russia Vocational Training College No.1, Xuan Hoa, Phu Tho, Vietnam*

Correspondence

H. T. HUNG, Department of Physics, Hanoi Pedagogical University 2, Xuan Hoa, Phu Tho, Vietnam

Email: hathanhhung@hpu2.edu.vn

History
- Received: 13-03-2025
- Accepted: 09-08-2025
- Published Online: 24-10-2025

DOI :
https://doi.org/10.32508/stdj.v28i4.4438

INTRODUCTION ABOUT 331 ISS

After the Higgs boson was experimentally shown to exist with certainty (5σ of CL-Confident Level), lepton flavor violation processes received more attention[1,2]. In particular, the decay channels violate the flavor number of particles are evidenced through the mass and oscillations of neutrinos and their constraints are established at accelerators[3,4].

$$Br(\mu \to e\gamma) < 4.2 \times 10^{-13},\quad Br(\tau \to e\gamma) < 3.3 \times 10^{-8},\quad Br(\tau \to \mu\gamma) < 4.4 \times 10^{-8}. \qquad Eq.(1)$$

Although, there is not yet enough reliable evidence to indicate the oscillation of charged leptons, the hypothesis of its existence has explained many new physical phenomena such as: nucleon transformation processes in nuclear matter, transformation processes of K, B-mesons, contribution to g-2 of muons...[5–7]
Following that approach, many models have been built to study the lepton flavor violation processes. Among them, the 331 models have achieved many outstanding advantages as follows: i) the number of particles is not too large and contains natural mass hierarchy[8,9], ii) many mechanisms can be applied to generate mass and explain the oscillation of neutrinos[5,10], iii) there is a large source of lepton flavor violation when applying seesaw mechanism[10,11], iv) easily satisfies the experimental limits of some basic decay processes…[9,12]
Therefore, in this work we use the 331 ISS model with the following characteristics:
The particles in the model are arranged based on the symmetry group $SU(3)_C \otimes SU(3)_L \otimes U(1)_X$ with the following rules: *i*) left-handed particles are placed in the triplets of the $SU(3)_L$ group *ii*) right-handed particles are placed in the singlets of $SU(3)_L$.
There are three exotic leptons located at the base of the $SU(3)_L$ triplets, which have no right-handed component due to $(N'_a)^C_L = (N'_a)_R$[10].

$$L'_{aL} = \begin{pmatrix} \nu'_a \\ l'_a \\ (N'_a)^c \end{pmatrix}_L : (1,3,-1/3),\ l'_{aR} : (1,1,-1) \quad Eq.(2)$$

To ensure chiral anomaly suppression, the left-handed quarks are placed in two antitriplets and one triplet of the $SU(3)_L$ group.

$$Q'_{\alpha L} = \begin{pmatrix} d'_\alpha \\ -u'_\alpha \\ D'_\alpha \end{pmatrix}_L : (3,3*,0), \begin{cases} d'_{\alpha R} : (3,1,-1/3) \\ u'_{\alpha R} : (3,1,2/3) \\ D'_{\alpha R} : (3,1,-1/3) \end{cases} \qquad Eq.(3)$$
$$Q'^3_L = \begin{pmatrix} u'_3 \\ d'_3 \\ U' \end{pmatrix}_L : (3,3,1/3), \begin{cases} u'_{3R} : (3,1,2/3) \\ d'_{3R} : (3,1,-1/3) \\ U'_R : (3,1,2/3) \end{cases}$$

Cite this article : T. HUNG H, T. T. HANG N, T .GIANG P. **The contributing components of BR $(\mu \to e\gamma)$ in the 3-3-1 model with inverse seesaw neutrinos**. *Sci. Tech. Dev. J.* 2025; 28(4):3849-3856.

We use the denotes $i = 1, 2, 3, \alpha = 1,2$ and the prime to distinguish the initial states of the fermions. The quantum numbers corresponding to the components of the gauge group are given in parentheses next to the particles.

To generate mass for the particles, the model needs three scalar triplets.

$$\eta = \begin{pmatrix} \eta_1^0 \\ \eta_2^- \\ \eta_3^0 \end{pmatrix} : (1,3,-1/3),\ \rho = \begin{pmatrix} \rho_1^+ \\ \rho_2^0 \\ \rho_3^+ \end{pmatrix} : (1,3,2/3),\ \chi = \begin{pmatrix} \chi_1^0 \\ \chi_2^- \\ \chi_3^0 \end{pmatrix} : (1,3,-1/3)\ Eq.(4)$$

With VEVs introduced as follows:

$$\eta_1^0 = \frac{1}{\sqrt{2}}(v_1 + R_1 + iI_1),\ \eta_3^0 = \frac{1}{\sqrt{2}}(R_1' + iI_1'),\ \rho_2^0 = \frac{1}{\sqrt{2}}(v_2 + R_2 + iI_2),$$
$$\chi_1^0 = \frac{1}{\sqrt{2}}(R_3' + iI_3'),\ \chi_3^0 = \frac{1}{\sqrt{2}}(v_3 + R_3 + iI_3) \qquad Eq.(5)$$

Using the form of VEVs as in Eq.(5), most of the original fermions get masses at tree level[4,7,8]. Furthermore, both η_3^0 and χ_1^0 are canceled their VEVs, which reduces the free parameters in the model and, more importantly, it leads to a very natural inverse seesaw mechanism.

To use the inverse seesaw mechanism, three additional singletons of the gauge group, denoted $\chi_i,\ i = 1, 2, 3,$, are introduced. The Yukawa Lagrangian then takes the following form:

$$-L^Y = h_{ij}^e \overline{L_{iL}'}\rho l_{jR}' - h_{ij}^{\nu}\varepsilon^{mnp}\overline{(L_{iL}')_m}(L_{jL}')_n^c\rho_p^* + Y_{ij}\overline{L_{iL}'}\chi X_{jR}' + \frac{1}{2}(\mu_F)_{ij}\overline{(X_{iR}')^c}X_{jR}' + H.c.\ Eq.(6)$$

Although η and χ play the same role in the structure of the Lagrangian as Eq.(6), since they have the same quantum numbers. To eliminate the unwanted mixing between ν and the heavy singlets X_R, in the third term of Eq.(6) only appears while the structure with η is eliminated. Combined with $\eta_3^0 = \chi_1^0 = 0$ as mentioned in Eq.(5), we can use the formulas of the inverted seesaw mechanism to indicate the mass of the neutrinos [13].

The Higgs potential in its simplest form (as discussed[6,10]) is given as:

$$V_H = \mu_1^2(\rho^\dagger\rho + \eta^\dagger\eta) + \mu_2^2\chi^\dagger\chi + \lambda_1(\rho^\dagger\rho + \eta^\dagger\eta)^2 + \lambda_2(\chi^\dagger\chi)^2 + \lambda_3(\rho^\dagger\rho + \eta^\dagger\eta)(\chi^\dagger\chi) - \sqrt{2}f(\varepsilon_{ijk}\eta^i\rho^j\chi^k + H.c.)\ Eq.(7)$$

According to Eq.(4,5,7), this model will give three CP-even Higgs bosons with the lightest being identical to the corresponding one in the standard model. The detailed analysis has been mentioned in Ref.10, we ignore the neutral Higgs bosons because they do not participate in the processes here. In this work, we are only interested in the interactions of the charged Higgs bosons, whose masses and states are given as follows:

$$\begin{pmatrix} \rho_1^\pm \\ \eta_2^\pm \end{pmatrix} = \frac{1}{\sqrt{2}}\begin{pmatrix} -1 & 1 \\ 1 & 1 \end{pmatrix}\begin{pmatrix} G_W^\pm \\ H_1^\pm \end{pmatrix},\ \begin{pmatrix} \rho_3^\pm \\ \chi_2^\pm \end{pmatrix} = \begin{pmatrix} -s_\alpha & c_\alpha \\ c_\alpha & s_\alpha \end{pmatrix}\begin{pmatrix} G_Y^\pm \\ H_2^\pm \end{pmatrix}\ Eq.(8)$$

and

$$m_{H_1^\pm}^2 = 2fv_3,\ m_{H_2^\pm}^2 = 2fv_3(1 + t_\alpha^2), \quad Eq.(9)$$

where $s_\alpha = \sin\alpha,\ c_\alpha = \cos\alpha,\ t_\alpha = \tan\alpha = \frac{v_2}{v_3}$

Gauge bosons get their mass from the kinetic term of the scalar field $L_S^{kin} = \sum_{\phi=\eta,\rho,\chi}(D_\mu\phi)^+(D_\mu\phi)$, so, we have:

$$W_\mu^\pm = \frac{W_\mu^1 \mp iW_\mu^2}{\sqrt{2}},\ m_W^2 = \frac{g^2}{4}(v_1^2 + v_2^2)$$
$$Eq.(10)$$
$$Y_\mu^\pm = \frac{W_\mu^6 \pm iW_\mu^7}{\sqrt{2}},\ m_Y^2 = \frac{g^2}{4}(v_2^2 + v_3^2)$$

The paper is arranged as follows. In the next section, we apply the inverse seesaw mechanism and show the couplings that violate the lepton flavor number. We give the analytical form of the components contributing to decay in Section III. Numerical results are discussed in Section IV. Conclusions are in Section V.

INVERSE SEESAW MECHANISM AND COUPLINGS RELEVANT TO $\mu \to e\gamma$ DECAY

We derive from Eq.(6) to generate the masses for the neutrinos according to the inverse seesaw mechanism (ISS), the last two terms describing the mixing of the masses of the heavy neutrinos N_i and X_i. We introduce the new bases:

$$n_{pL}' = \left\{\upsilon_{iL}', N_{iL}', (X_{iR}')^C\right\}^T,\ (n_{pL}')^C = \left\{(\upsilon_{iL}')^C, (N_{iL}')^C, X_{iR}'\right\}^T,\ p = \overline{1,9}\ Eq.(11)$$

herefore, the mass term of neutrinos is:

$$-L_{mass}^{\nu} = \frac{1}{2}\overline{n_L'}M^\nu(n_L')^c + H.c.,\ with\ M^\nu = \begin{pmatrix} 0 & m_D & 0 \\ m_D^T & 0 & M_R^T \\ 0 & M_R & \mu_F \end{pmatrix}\ Eq.(12)$$

We put into the denotes:

$M^{\nu} = \begin{pmatrix} 0 & M_D \\ M_D^T & M_N \end{pmatrix}$, $where\ M_D \equiv (m_D,\, 0),\ M_N = \begin{pmatrix} 0 & M_R^T \\ M_R & \mu_F \end{pmatrix}$ $Eq.(13)$

Technically, to get the mass eigenvalues of the neutrinos we introduce a 9x) unitary matrix U^{υ}.

$U^{\upsilon T} M^{\upsilon} U^{\upsilon} = \widehat{M}^{\upsilon} = diag(m_{n_1},\, m_{n_2}, ..., m_{n_9}) = diag(\widehat{m}_{\upsilon},\, \widehat{M}_N).\ Eq.(14)$

Then, the relationship between the eigenstates and the initial state is:

$n'_L = U^{\nu *} n_L,\ (n'_L)^c = U^{\nu} (n_L)^c,\ or$

$P_L n'_P = n'_{pL} = U^{\nu *}_{pq} n_{qL},\ P_R n'_P = n'_{pR} = U^{\nu}_{pq} n_{pR},\ p.q = 1, 2, ..., 9.\ Eq.(15)$

The U matrix is parameterized in the following form [12,14]:

$U^{\nu} = \Omega \begin{pmatrix} U & O \\ O & V \end{pmatrix}$, $where\ \Omega = exp \begin{pmatrix} O & R \\ -R^{\dagger} & O \end{pmatrix} = \begin{pmatrix} 1 - \frac{1}{2} R R^{\dagger} & R \\ -R^{\dagger} & 1 - \frac{1}{2} R^{\dagger} R \end{pmatrix}$ $Eq.(16)$

with U chosen to be identical to U^{PMNS} according to Refs.14, 15, 16 [12,15,16] and of the form:

$$U^{PMNS} = \begin{pmatrix} c_{12}c_{13} & s_{12}c_{13} & s_{13}e^{-i\delta} \\ -s_{12}c_{13} - c_{12}s_{23}s_{13}e^{i\delta} & c_{12}c_{23} - s_{12}s_{23}s_{13}e^{i\delta} & s_{23}c_{13} \\ s_{12}s_{23} - c_{12}c_{23}s_{13}e^{i\delta} & -c_{12}s_{23} - s_{12}c_{23}s_{13}e^{i\delta} & c_{23}c_{13} \end{pmatrix} diag\left(1, e^{i\frac{\sigma_1}{2}}, e^{i\frac{\sigma_2}{2}}\right)\ Eq.(17)$$

We also use additional formulas related to ISS mechanism [14,15,16].

$R^* = \left(-m_D M^{-1} \quad m_D (M_R\ )^{-1} \right),\ m_D M^{-1} m_D^T = m_{\nu} \equiv U^*_{PMNS} \widehat{m}_{\nu} U^{\dagger}_{PMNS},$

$V^* \widehat{M}_N V^{\dagger} = M_N + \frac{1}{2} R^T R^* M_N + \frac{1}{2} M_N R^{\dagger} R,\ M \equiv M_R^T \mu_F^{-1} M_R\ Eq.(18)$

To satisfy the above conditions, can be chosen to be antisymmetric and the trace elements to be zero, combined with the experimental data of neutrinos and the choice of Dirac phase [17,18], we can parametrize as follows [10]:

$$m_D = k \times \begin{pmatrix} 0 & 1 & 0.7248 \\ -1 & 0 & 1.8338 \\ -0.7248 & -1.8338 & 0 \end{pmatrix}\ Eq.(19)$$

with $k = \sqrt{2} v_2 h^{\nu}_{ij}$ depending on the lepton masses and having an upper bound of 617 GeV.

Based on the Yukawa Lagrangian in Eq.(6), we derive the interactions of the charged Higgs bosons, applied to the first term as:

$$-h^e_{ij} \overline{L'_{iL}} \rho l'_{jR} + h.c. = -\frac{g m_i}{m_W} \left[\overline{\nu'_{iL}} l'_{iR} \rho_1^+ + \overline{l'_{iL}} l'_{iR} \rho_2^0 + \overline{N'_{iL}} l'_{iR} \rho_3^+ + h.c. \right]$$

$$\supset -\frac{g m_i}{\sqrt{2} m_W} \left[\left(U^{\nu}_{ip} \overline{n_P} P_R l_i H_1^+ + U^{\nu *}_{ip} \overline{l_i} P_L n_P H_1^- \right) \right]$$

$$-\frac{g m_i}{m_W} \left[c\alpha \left(U^{\nu}_{(i+3)i} \overline{n_P} P_R l_i H_2^+ + U^{\nu *}_{(i+3)p} \overline{l_i} P_L n_P H_2^- \right) \right]\ Eq.(20)$$

The result obtained when applied to the second term is:

$$h^{\nu}_{ij} \varepsilon^{npk} \overline{(L'_{iL})}_n \left(L'_{jL} \right)^c_p \rho^*_k + h.c. = 2 h^{\nu}_{ij} \left[-\overline{l'_{iL}} \left(\nu'_{jL} \right)^c \rho_3^- - \overline{\nu'_{iL}} \left(N'_{jL} \right)^c \rho_2^{0*} + \overline{l'_{iL}} \left(N'_{jL} \right)^c \rho_1^- \right]$$

$$\supset -\frac{g c_{\alpha}}{m_W} \left[(m_D)_{ij} U^{\nu}_{ip} H_2^- \overline{l_i} P_R n_P + h.c. \right] - \frac{g}{\sqrt{2} m_W} \left[(m_D)_{ij} U^{\nu}_{(j+3)p} H_1^- \overline{l_i} P_R n_P + h.c. \right] Eq.(21)$$

The result obtained when applied to the third term is:

$$-Y_{ab} \overline{L'_{aL}} \chi X'_{bR} + h.c. = -\frac{\sqrt{2}}{w} (M_R)_{ab} \left[\overline{\nu'_{aL}} \chi_1^0 + \overline{L'_{aL}} \chi_2^- + \overline{N'_{aL}} \chi_3^0 \right] X'_{bR} + h.c.$$

$$\supset -\frac{g t_{\alpha}}{\sqrt{2} m_W} (M_R)_{ij} \left[\sqrt{2} s_{\alpha} U^{\nu}_{(j+6)p} \overline{l_i} P_R n_P H_2^- + h.c. \right]\ Eq.(22)$$

The couplings of charged gauge bosons is given by the kinetic energy term of the leptons.

$$L^{eeV} = \overline{L'_{iL}} \gamma^{\mu} D_{\mu} L'_{iL} \supset \frac{g}{\sqrt{2}} \left(\overline{l'_{iL}} \gamma^{\mu} \nu'_{iL} W^-_{\mu} + \overline{l'_{iL}} \gamma^{\mu} N'_{iL} Y^-_{\mu} \right) + h.c = \frac{g}{\sqrt{2}}$$

$$\left[U^{\nu *}_{ip} \overline{l_i} \gamma^{\mu} P_L n_P W^-_{\mu} + U^{\nu}_{ip} \overline{n_P} \gamma^{\mu} P_L l_i W^+_{\mu} + U^{\nu *}_{(i+3)p} \overline{l_i} \gamma^{\mu} P_L n_P Y^-_{\mu} U^{\nu}_{(i+3)p} \overline{n_P} \gamma^{\mu} P_L l_i Y^+_{\mu} \right]\ Eq.(23)$$

We use assignment as follows [10]:

$\lambda^{L,1}_{i,p} = -\sum_{k=1}^{3} (m^*_D) U^{\nu *}_{(k+3)p}, \qquad \lambda^{R,1}_{i,p} = m_i U^{\nu}_{ip}$

$\lambda^{L,2}_{i,p} = -\sum_{k=1}^{3} \left[(m^*_D)_{ip} U^{\nu *}_{kp} + t^2_{\alpha} (M^*_R)_{ip} U^{\nu *}_{(k+6)p} \right],\ \lambda^{R,2}_{i,p} = m_i U^{\nu}_{(i+3)p}\ Eq.(24)$

The lepton-flavor-violating couplings involved in $\mu \to e\gamma$ decay are given in Table 1:

Based on the couplings in Table 1, we derive the contribution diagrams for $\mu \to e\gamma$ as shown in Figure 1. Among the decays of charged leptons as mentioned in Eq.(1), $BR(\mu \to e\gamma)$ has the strictest experimental bounds. It means that the parameter space regions satisfying the experimental bounds of this decay channel also satisfy the decay channels of the same type($\tau \to e\gamma$ and $\tau \to \mu\gamma$) [6,10]. Furthermore, the contributions to the $\tau \to e\gamma$ and $\tau \to \mu\gamma$ decay channels are also expressed analytically in a similar way to $\mu \to e\gamma$. Therefore, in this work we only study the contributions to $\mu \to e\gamma$ and show the parameter space regions satisfying its

Table 1: The couplings are related to $l_i \to l_j\gamma$ decays in the unitary gauge. All momentumat the vertices is considered to be incoming.

Vertex	Coupling	Vertex	Coupling
$\bar{n}_p e_i H_1^+$	$-\frac{ig}{\sqrt{2}m_W}\left(\lambda_{ip}^{R,1}P_R+\lambda_{ip}^{L,1}P_L\right)$	$\overline{e}_i n_p H_1^-$	$-\frac{ig}{\sqrt{2}m_W}\left(\lambda_{ip}^{*L,1}P_R+\lambda_{ip}^{*R,1}P_L\right)$
$\bar{n}_p e_i H_2^+$	$-\frac{igc_\alpha}{m_W}\left(\lambda_{ip}^{R,2}P_R+\lambda_{ip}^{L,2}P_L\right)$	$\overline{e}_i n_p H_2^-$	$-\frac{igc_\alpha}{m_W}\left(\lambda_{ip}^{*L,2}P_R+\lambda_{ip}^{*R,2}P_L\right)$
$\bar{n}_p e_i Y_\mu^+$	$\frac{ig}{\sqrt{2}}U^{L*}_{(i+3)p}\gamma^\mu P_L$	$\overline{e}_i n_p Y_\mu^-$	$\frac{ig}{\sqrt{2}}U^{L}_{(i+3)p}\gamma^\mu P_L$
$\bar{n}_p e_i W_\mu^+$	$\frac{ig}{\sqrt{2}}U^{L*}_{ip}\gamma^\mu P_L$	$\overline{e}_i n_p W_\mu^-$	$\frac{ig}{\sqrt{2}}U^{L}_{ip}\gamma^\mu P_L$

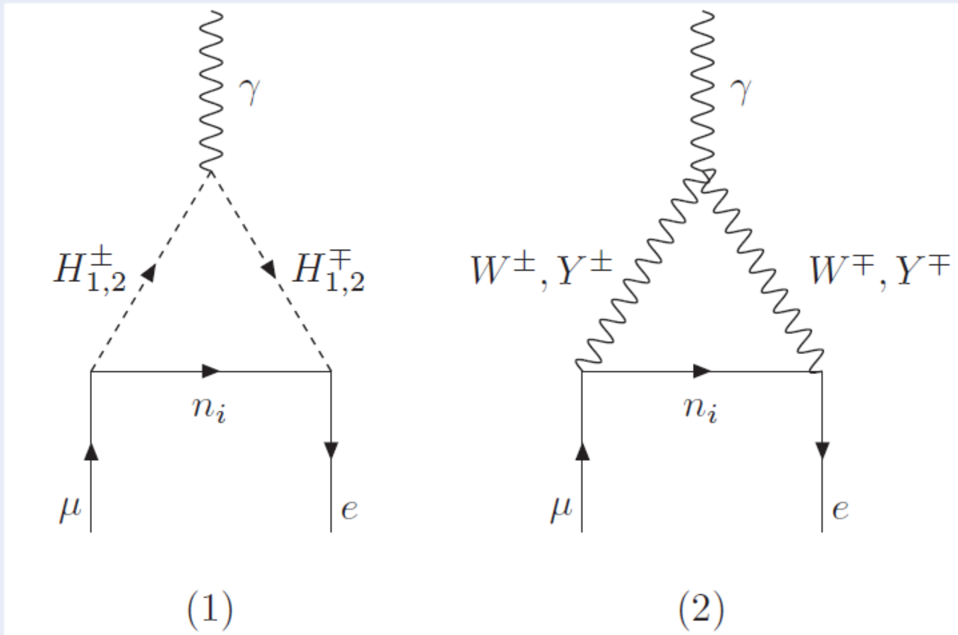

Figure 1: All Feynman diagrams of $\mu \to e\gamma$ process in gauge unitary.

experimental bounds. These parameter space regions will automatically satisfy the decay channels $BR(\tau \to e\gamma)$ and $BR(\tau \to \mu\gamma)$ [10].

COMPONENTS CONTRIBUTING TO $\mu \to e\gamma$ DECAY.

In general, the branching ratio of $l_i \to l_j\gamma$ is given [19,20].

$Br(l_i \to l_j\gamma) = \frac{12\pi^2}{G_F^2}\left(|C_L|^2 + |C_R|^2\right)Br(l_i \to l_j\overline{\nu_j}\nu_i), \quad Eq.(25)$

with $\mu \to e\gamma$ we have $BR(\mu \to e\overline{\nu_e}\nu_\mu) = 100\%$ and $m_{\mu,e} = 1.0\,TeV$ then we can ignore $C_L\,(C_L = C_R)$ [6,21,22], so the branching ratio of this decay channel is rewritten as:

$BR(\mu \to e\gamma) = \frac{12\pi^2}{G_F^2}|C_R|^2, \qquad Eq.(26)$

The contributions corresponding to diagram (1) in Figure 1 are:

$$C_R^{H_s^\pm} = -\frac{eg^2c_s}{16\pi^2m_W^2}\sum_{p=1}^{9}\left[\frac{\lambda_{1p}^{L,S*}\lambda_{2p}^{L,S}}{m^2_{H_s^\pm}}\times\frac{1-6t_{ps}+3t_{ps}^2+2t_{ps}^3-6t_{ks}^2\ln(t_{ks})}{12(t_{ps}-1)^4}+\frac{m_{n_p}\lambda_{1p}^{L,S*}\lambda_{2p}^{\prime R,S}}{m^2_{H_s^\pm}}\times\frac{-1+t_{ps}^2-2t_{ps}\ln(t_{ps})}{2(t_{ps}-1)^3}\right], \; Eq.(27)$$

where $s = 1,2,\; c_1 = c_\alpha^2,\; c_2 = \frac{1}{2}$ and $t_{ps} = \frac{m^2_{n_p}}{m^2_{H_s^\pm}}$

The contributions corresponding to diagram (2) in Figure 1 are:

$$C_R^{W^\pm} = -\frac{eg^2}{32\pi^2m_W^2}\sum_{p=1}^{9}U_{2p}^{\nu*}U_{1p}^{\nu}F\left(t_{pW}\right),$$

$$Eq.(28)$$

$$C_R^{Y^\pm} = -\frac{eg^2}{32\pi^2m_Y^2}\sum_{p=1}^{9}U_{5p}^{\nu*}U_{4p}^{\nu}F\left(t_{pY}\right),$$

where $t_{pW} = \frac{m^2_{n_p}}{m^2_{W^\pm}}$ and $t_{pY} = \frac{m^2_{n_p}}{m^2_{Y^\pm}}$

The function F(t) is derived as [6,10]

$$F(t) \equiv \frac{10 - 43t + 78t^2 - 49t^3 + 4t^4 + 18t^3 \ln(t)}{12(t-1)^4} \quad Eq.(29)$$

NUMERICAL RESULTS

We use the well-known experimental parameters [1,2,23,24]: the charged lepton masses $m_\tau = 1.776GeV, m_\mu = 0.105GeV$, $m_e = 5.10^{-4}GeV$ the SM-like Higgs boson mass $m_{h_1^0} = 125,09GeV$, the mass of the W boson $m_W = 80.385GeV$ and the gauge coupling of the $SU(2)_L$ symmetry $g = 0.651$.

We also include fixed values based on known experimental limits [6,10] as:

$m_Y = 4.5\ TeV, m_{H_1^\pm} \geq 500\ GeV, M_R = k \times diag(1,1,1)$.

To perform the numerical calculation, we use the experimental data on neutrino oscillations [1,2,25] for Eq.(17),

$$s^2_{12} = 0.32,\ s^2_{23} = 0.551,\ s^2_{13} = 0.0216, \qquad Eq.(30)$$
$$\triangle m^2_{21} = 7.55 \times 10^{-5} eV^2,\ \triangle m^2_{32} = 2.50 \times 10^{-3} eV^2,$$

and apply Eq.(19) to parameterize m_D. The result is that $C_R^{W^\pm}, C_R^{Y^\pm}, C_R^{H_1^\pm}, C_R^{H_2^\pm}$ depend only on two parameters k and $m_{H_2^\pm}$. The dependence of the components contributing to $BR(\mu \to e\gamma)$ on the parameters k and $m_{H_2^\pm}$ are given in Figure 2 and Figure 3, respectively.

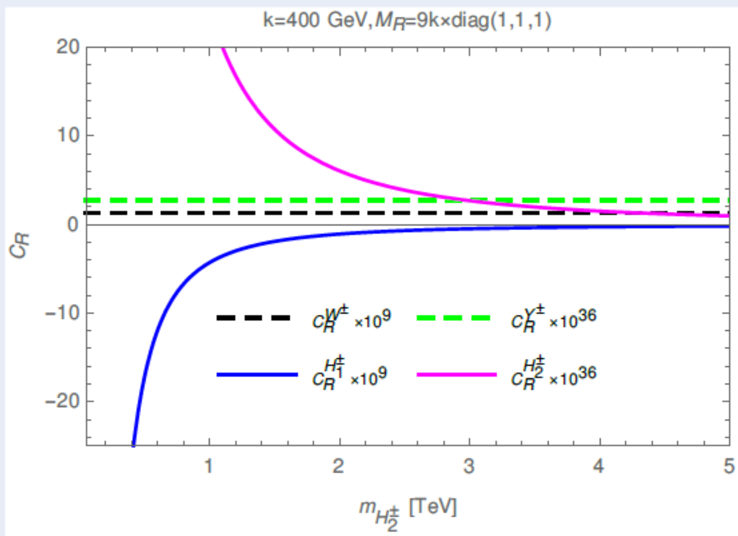

Figure 2: Contributors to $\mu \to e\gamma$ decay depend on $m_{H_2^\pm}$ in the case $k = 400\ GeV$ and $M_R = k \times diag(1,1,1)$.

The results obtained in Figure 2 and Figure 3 have the following common characteristics: *i)* $C_R^{W^\pm}$, $C_R^{H_1^\pm}$ have the same size 10^{-9} *ii)* $C_R^{Y^\pm}$, $C_R^{H_2^\pm}$ have the same size 10^{-36} *iii)* $C_R^{W^\pm}$, $C_R^{Y^\pm}$ are always positive, very small and does not change with the variable k(or $m_{H_2^\pm}$) *iv)* $C_R^{H_1^\pm}$, $C_R^{H_2^\pm}$ changes very quickly and with the opposite sign with the variable k (or $m_{H_2^\pm}$).

The biggest difference between Figure 2 and Figure 3 is that while the magnitudes of $C_R^{H_1^\pm}$ and $C_R^{H_2^\pm}$ decrease with $m_{H_2^\pm}$ (Figure 2), they increase with k (Figure 3). Furthermore, the numerical investigations in Figure 2 and Figure 3 provide a comprehensive comparison of the contributions of $BR(\mu \to e\gamma)$, both in sign and magnitude. This is a new result compared to what was presented in Refs.7, 9, 10, leading to the identification of a more suitable parameter space for studying other LFV processes. The features of $C_R^{W^\pm}, C_R^{H_1^\pm}, C_R^{Y^\pm}, C_R^{H_2^\pm}$ as mention above, create interference between the components contributing to $BR(\mu \to e\gamma)$. This also explains the regions of parameter space that satisfy the experimental limit of $BR(\mu \to e\gamma)$ (<4.2 x 10^{-13}) that are formed by the resonance of the above interference. We show this result in Figure 4.

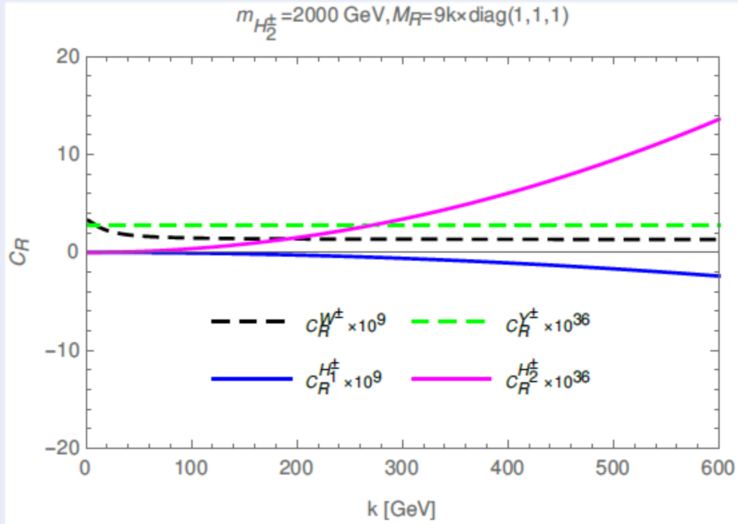

Figure 3: Contributors to $\mu \to e\gamma$ decay depend on k in the case $m_{H_2^\pm} = 2000\ GeV$ and $M_R = 9k \times diag(1,1,1)$.

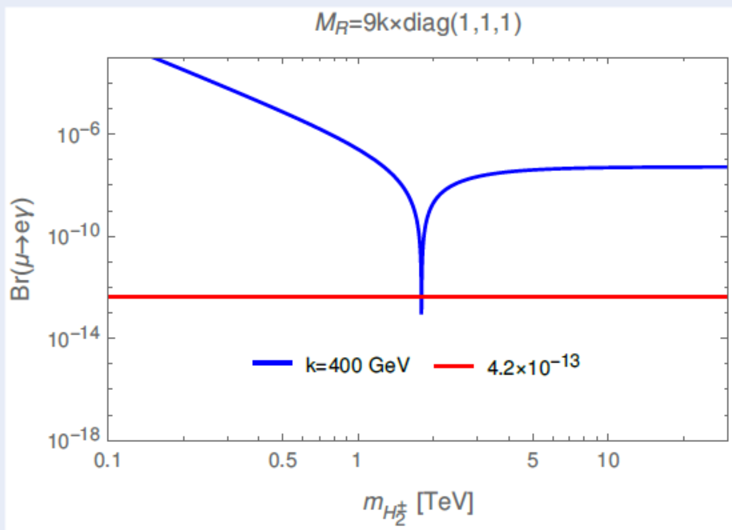

Figure 4: Plot of $BR(\mu \to e\gamma)$ depend on $m_{H_2^\pm}$ in the case $k = 400\ GeV$ and $M_R = 9k \times diag(1,1,1)$.

The allowed parameter space is depicted as the blue part below the red line in Figure 4. To be more specific, we will represent it on $\left(m_{H_2^\pm}, k\right)$ plane. The result is shown in Figure 5 the space that satisfies the experimental limit of $BR(\mu \to e\gamma)$ is the colorless part, the green part corresponds to $4.2 \times 10^{-13} < BR(\mu \to e\gamma) < 300 \times 10^{-13}$, the yellow part corresponds to $300 \times 10^{-13} < BR(\mu \to e\gamma) < 600 \times 10^{-13}$ and the cyan part corresponds to $BR(\mu \to e\gamma) > 600 \times 10^{-13}$. The allowed space region in Figure 5 can be used to study other physical processes such as: Lepton flavor violating decay of SM-likes Higgs bosons, neutron transition in nuclear matter ($CR\left(\mu^- Ti \to e^- Ti\right)$), complement to anomalous magnetic moment (g-2) of muon, lepton flavor violating decay of K (B)-meson...

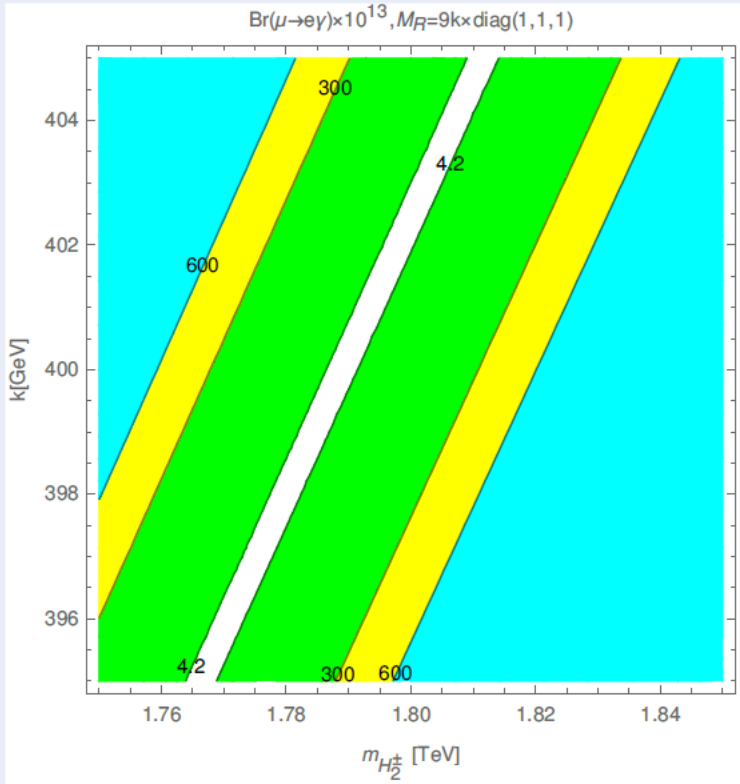

Figure 5: Contour plot of $\mu \to e\gamma$ decay on the plane $\left(m_{H_2^{\pm}}\ ,\ k\right)$. The areas parameter satisfies experimental limits is colorless.

CONCLUSIONS

We use the inverse seesaw mechanism to generate mass for the active neutrinos in 331 ISS. The consequence is that it gives this model a large source of lepton flavor violation which allows us to study $\mu \to e\gamma$ decay. We have established an analytical form for the contributions to $BR(\mu \to e\gamma)$ of charged bosons $\left(W^{\pm},\, Y^{\pm},\, H_1^{\pm},\, H_2^{\pm}\right)$ at one-loop order.

The interpretation of the experimental data of active neutrinos and other experimental constraints allows us to fix the parameters of the model, resulting in $BR(\mu \to e\gamma)$ depending only on k and $m_{H_2^{\pm}}$. By numerical investigation, we compare the strengths of the components contributing to $BR(\mu \to e\gamma)$ and show that theparameter space region of the model satisfies the experimental constraints of $BR(\mu \to e\gamma)$.

CONFLICT OF INTERESTS

The authors declare that they have no known competing financial interests or personal relationships that could have appeared to influence the work reported in this paper.

AUTHORS' CONTRIBUTIONS

H. T. Hung: investisgate numerical, discuss and write the contents.
N.T.T.Hang: establish analytic formulas for decays of charged lepton.
P.T.Giang: brief review of the model and establish LFV couplings.

ACKNOWLEDGEMENTS

This research is funded by the Foundation for Science and Technology Development, Hanoi Pedagogical University 2 via grant number HPU2.2022-UT-04.

REFERENCES

1. Chatrchyan S, CMS collaboration . Physics Letters [Part B]. 2012;716:30. Available from: http://doi.org/10.1016/j.physletb.2012.08.021.
2. ATLAS collaboration GA, et al. Observation of a new particle in the search for the Standard Model Higgs boson with the ATLAS detector at the LHC. PhysLett . 2012;B716:1–29.
3. Patrignani C, et al. Review of Particle Physics. Chinese Physics (Beijing). 2016;C40(10).
4. Zyla PA, et al. The Review of Particle Physics . PTEP. 2020;083C01.
5. Dong PV, Long HN. Neutrino masses and lepton flavor violation in the 3-3-1 model with right-handed neutrinos. Physical Review D: Particles, Fields, Gravitation, and Cosmology. 2012;77(5). Available from: http://doi.org/10.1103/PhysRevD.77.057302.
6. Hue LT, Ninh LD, Thuc TT, Dat NTT. Exact one-loop results for l_i $\to l\_j\gamma in 3-3-1 models. Eur Phys J. 2018; C78(128).$
7. Hue LT, Hung HT, Tham NT, Long HN, Nguyen TP. Large (g $-$ 2)_μ and signals of decays e_b $\to$ e_aγ in a 3 $-$ 3 $-$ 1 model with inverse seesaw neutrinos. Phys RevD. 2021;D104(033007). Available from: http://doi.org/10.1103/PhysRevD.104.033007.
8. Chang D, Long HN. Interesting radiative patterns of neutrino mass in an SU (3) C ∅times SU (3) L ∅times U (1) X model with right-handed neutrinos. Physical Review D: Particles, Fields, Gravitation, and Cosmology. 2006;73(5). Available from: http://doi.org/10.1103/PhysRevD.73.053006.
9. Hue LT, Khoi DP, Phuong HH, Hung HT. Lepton Flavor Violation in Economical 3-3-1 Model with Neutrino Singlets. Communications on Physics. 2019;29(1):87–96. Available from: http://doi.org/10.15625/0868-3166/29/1/13556.
10. Hung HT, Tham NT, Hieu TT, Hang NTT. Contribution of heavy neutrinos to decay of standard-model-like Higgs boson in a 3-3-1 model with additional gauge singlets. PTEP. 2021;083B01(2103):16018. Available from: https://doi.org/10.1093/ptep/ptab082.
11. Hong TT, Hung HT, Phuong HH, Phuong LTT, Hue LT. Lepton-flavor-violating decays of the SM-like Higgs boson h $\to$ e i e j h$\to$e i e j , and e i $\to$ e j γ e i $\to$e j γ in a flipped 3-3-1 model. PTEP. 2020;4(043B03):06826. Available from: http://doi.org/10.1093/ptep/ptaa026.
12. Hung HT, Hong TT, Phuong HH, Mai HL, Hue LT. Neutral Higgs boson decays H °ightarrow Z γ, $\gamma\,\gamma$ in 3-3-1 models. Physical Review D. 2019;100(7).
13. Catano ME, Martínez R, Ochoa F. Neutrino masses in a 331 model with right-handed neutrinos without doubly charged Higgs. PhysRev . 2012;D86(073015). Available from: https://doi.org/10.48550/arXiv.1206.1966.
14. Ibarra A, Molinaro E, Petcov ST. TeV scale see-saw mechanisms of neutrino mass generation, the Majorana nature of the heavy singlet neutrinos and $(\beta\beta)0\nu$-decay. The Journal of High Energy Physics. 2010;1009(9):108.
15. Maki Z, Nakagawa M, Sakata S. Remarks on the Unified Model of Elementary Particles. Progress of Theoretical Physics. 1962;28(5):870–80.
16. Pontecorvo B. Inverse Beta Processes and Nonconservation of Lepton Charge. Soviet Physics, JETP. 1958;7:172–173.
17. Okada H, Okada N, Orikasa Y, Yagyu K; 2016.
18. Kanemura S, Kikuchi M, Mawatari K, Sakurai K, Yagyu K; 2018.
19. Lavoura L. General formulae for $f_1 f_2 $. The European Physical Journal C. 2003;29(2):191–5.
20. Griffiths D. Introduction to elementary particles. Wiley-VCH Express; 1986.
21. ATLAS Collaboration GA, et al. Search for a Charged Higgs Boson Produced in the Vector-boson Fusion Mode with Decay using Collisions at TeV with the ATLAS Experiment. Rev Lett . 2015;114(231801). Available from: https://doi.org/10.48550/arXiv.1503.04233.
22. CMS Collaboration VK, et al. Search for a charged Higgs boson in pp collisions at sqrt(s) = 8 TeV. JHEP 11. 2015;018. Available from: https://doi.org/10.48550/arXiv.1508.07774.
23. CMS Collaboration AMS, et al. Search for high-mass resonances in dilepton final states in proton-proton collisions at 13 TeV. JHEP 06. 2018;120. Available from: https://doi.org/10.48550/arXiv.1803.06292.
24. Aad G, ATLAS Collaboration, et al. Search for high-mass dilepton resonances using 139 fb of collision data collected at 13 TeV with the ATLAS detector. Phys Lett . 2019;B796(68). Available from: https://doi.org/10.48550/arXiv.1903.06248.
25. Cepeda M, et al. Higgs Physics at the HL-LHC and HE-LHC. CERN Yellow Rep Monogr . 2019;7(221). Available from: https://doi.org/10.48550/arXiv.1902.00134.